文献2

Proceedings of International Symposium on Environmental-Conscious Innovative Materials Processing with Advanced Energy Sources (Ecomap-98), Nov.24-27, 1998, Kyoto, Japan

DEPOSITION METHOD USING ULTRAFINE PARTICLE BEAM AND ITS APPLICATIONS

JUN AKEDO

Mechanical Engineering Laboratory, A.I.S.T./M.I.T.I.,
Namiki, Tsukuba, Ibaraki,305-8564, JAPAN
E-mail : akedo@mel.go.jp

Abstract
Ultrafine particles (UFP) jetting with the velocities of several hundreds m/s is accumulated on the metal and ceramic substrate via impact adhesion. Recently, the application of this phenomenon for micro electro mechanical systems (MEMS) and micro devices has been investgated. In this paper, the deposition method based on ultra-fine particle beam and possibilities of its application are reported.

1. INTRODUCTION

Several deposition methods based on the principle of particle impaction have already been investgated. They include depositing ultrafine particles (UFP) via electrical field acceleration (Electrostatic Particle-Impact Deposition (EPID)[1]), and via acceleration by mixing with high speed gas flow (Gas Deposition Method (GDM)[2] or Hypersonic Plasma Particle Deposition (HPPD)[3]). The expected features of these methods are high speed depotion ratio and film formation at low temperature.

In the microactuators and ultrasonic devices needed for MEMS, etc. and in the miniaturized magnetic devices needed for mobile communication equipment, it is important to make piezoelectric ceramics and high-magnetic-permeability ceramics in the form of a thin film and to process it finely. By far, in order to match requirements, fabrication of these ceramics generally requires high-temperature heat treatment. On the other hand, for some applications, it is necessary to obtain a film with thickness in 1 to 100 μ m range[4]. However, in conventional techniques such as sputtering and sol-gel method, the processing time becomes too long and fine etching processing for these thick films is difficult sometimes. There are also problems in cutting ceramic pieces from the bulk material, and in handling and joining of membranes in the grinding-and-polishing process.

For these reasons, we study a new deposition technique based on impact adhesion of ultrafine particle beam for forming and micro-patterning thick functional ceramic layers. If the crystal structure of the ceramic particles is preserved during the deposition, the processes temprature might be decreased and the wide application of these methods is ex-

pected. GDM is the simplest method of energy supplement for the deposition among the methods discribed above. In GDM, individual particles of ceramic material having a diameter less than 0.5 μ m are mixed with a carrier gas and form colloiding gas flow, which is ejected from a micro orifice nozzle and deposited onto a substrate. It is said that collision of the UFP with the substrate converts part of kinetic energy of the flow to local thermal energy, and this promotes bonding between the substrate and the UFP and between the UFP themselves. Although, the actually mechanism has not been clarified yet. Recently, some reports about GDM for forming and patterning of thick films have been published[2],[5],[6] . We have already introduced GDM and improved its system to a jet molding system (JMS) [7] for the micro-fabrication of three dimensional structures of some metal materials and PZT. And we have also reported some properties of the deposited film in other reports[8],[9].

The purpose of this paper is to clarify the deposition properties of GDM in order to understand the deposition mechanism of this technique and improve the physical property. Some results of deposition of several functional ceramics, namely ultra-fine particles of PZT for sensing and actuation, ultra-fine particles of NiZn ferrite for soft magnetic material, and TiO2 for photocatalyst are described. All the ceramics films were deposited on Si, SUS,and Pt/Ti/SiO2/Si substrate by GDM and observed by XRD. Relationship of the ferroelectric property of PZT film with its microstructure is also referred.

2. EXPERIMENTAL RESULRTS AND DISCUSSION

2.1 Experimental setup and conditions

Figure 1 shows the constitution of our GDM apparatus. Our GDM apparatus has two vacuuming chambers connecting each other through a gas pipe. The first is the deposition chamber for the formation and patterning of films. It contains of the nozzle, substrate, and mask alignment system. This chamber is vacuumed during the deposition by a rotary vacuum pump and a mechanical booster pump. The second is aerosol chamber for generation of UFP aerosol. It has the carrier gas introducing system and vibration system. Fine ceramic powder contained in the aerosol chamber is delivered to the deposition chamber by pressure difference between the chambers and by vibration. The UFP ceramics powder is ejected through the micro orifice nozzle and deposited onto the substrate through laser-patterned masks. The apparatus in details has been described in the previous reports[7]. Table 1 shows the typical parameters of deposition condition for aerosol GDM. He (as a non-activated gas) or Air (as an oxidized gas) is used as the carrier gas. The pressure of the aerosol chamber is about 480 Torr, and that of the deposition chamber is 0.5～5 Torr in all deposition experiments. The orifice size of nozzle is 5mm×600 μ m, the relative veloc-

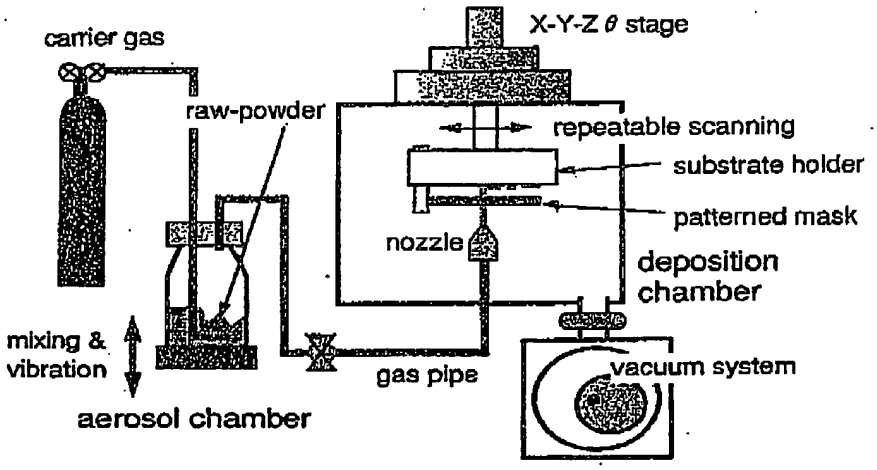

Figuer 1. Experimental setup of aerosol gas deposition method (schematically)

ity of the nozzle motion along the substrate is from 0.125 to 1.25mm ／ sec, and the distance between the nozzle and the substrate is from 2mm to 10mm. Under these conditions, the ejected gas flow speed reachs sonic speed. We used commercially available raw-powder of PZT having a perovskite structure with average particle diameter of 0.3 μ m and TiO2 having an anastuse structure with average particle diameter of 0.15 μ m. The raw-powder of NiZn ferrite having a spinel structure with average particle diameter of 0.3 μ m was prepared by solid-state reaction method at 800℃, 2h and ball-milling process.

	Typcal condition
pressure of the film-deposition chamber	0.5～5 Torr
pressure difference between two chambers	0.5 atm
distance between the nozzle and the mask	2～10mm
orifice size of nozzle	5mm×600 μm
relative velocity of the nozzle to the substrate	0.125～1.25 mm/s
substrate temperature	room temp.
average particle size	< 0.3 μm

Table 1. Typcal parameter of the deposition condition for aerosol GDM.

2.2 Film formation

Under these conditions, we have obtained PZT, NiZn ferrite, and TiO2 films deposited up to 100 μ m on Si and Stainless Steel (SUS304) in area 5mm × 5mm without peeling. The highest deposition ratio 16.7 μ m ／ min was reached for PZT. Figure 2 shows a micro-patterned PZT thick film which was produced by the mask deposition method with-

out etching. The adhsion forces of the deposited films at room temperature were measured by a tensile testing machine. As the result, all the experiments were finished by breakage of epoxy resin used for joining the samples to the machine holder at 20MPa. That means the deposited films have strong adhesion force higher than 20MPa on the Si and SUS substrates. In order to determine the density, the films were prepared with thickness more than 100 μ m. Volume and weight was obtained using a three-dimensional stylus profiler and a precise weight balance with the resolution of 10 μ g, respectively. The density of the PZT film was estimated to be 7.76g / cm^3, which is more than 95% of the bulk density (7.88 g / cm^3). It is difficult to explain such a strong adhesion force and high density of the deposited films by the kinetic energy transformation only, taking into account the size effect of particle diameter in the normal sintering process .

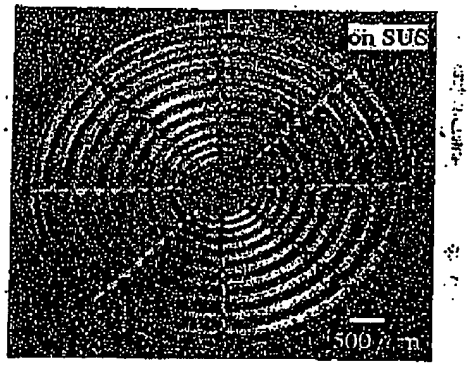

Figure 2. Thick PZT layer on the SUS substrate patterning by GDM.

2.3 Microstructure of the deposited film observed by SEM and XRD

Figures 3 (a),(b) show the SEM image of (a) raw-powder, (b) as-deposited film at room temperature. In Fig.3(a) each particle was separated and has a distinct particle boundary. In Fig.3(b) the single particles have no longer edge lines and are combined with each other. It looks, as if the condensation of the powders was induced in the deposition process.

Crystal structures of the deposited films have been observed by X-ray diffraction (XRD : Cu K-alpha, 40kV/120mA) through the comparison of samples before and after deposition. XRD profile of each sample is shown in Figures 4, Figures 5, Figures 6. Fig. 4 (a),

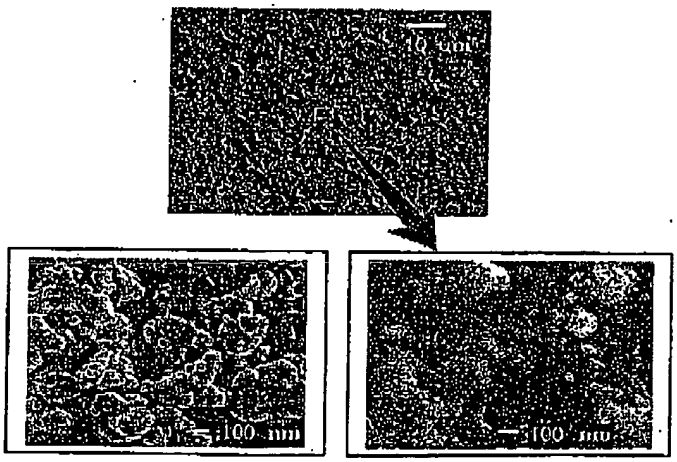

(a) raw-powder. (b) as-deposited film at room temperature.

Figure 3. SEM image of deposited PZT film.

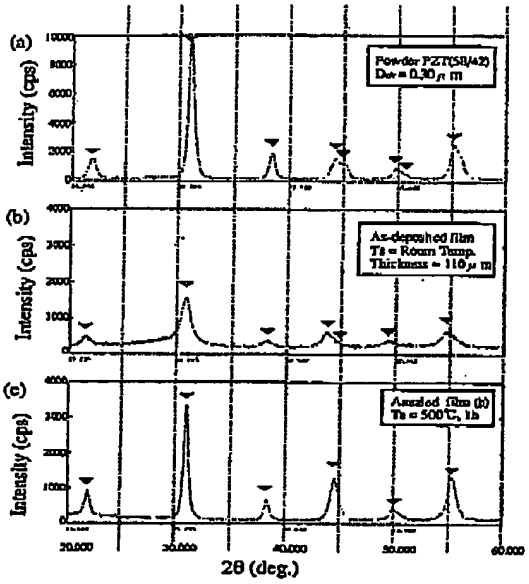

Figure 4. Comparison of XRD pattern of PZT.

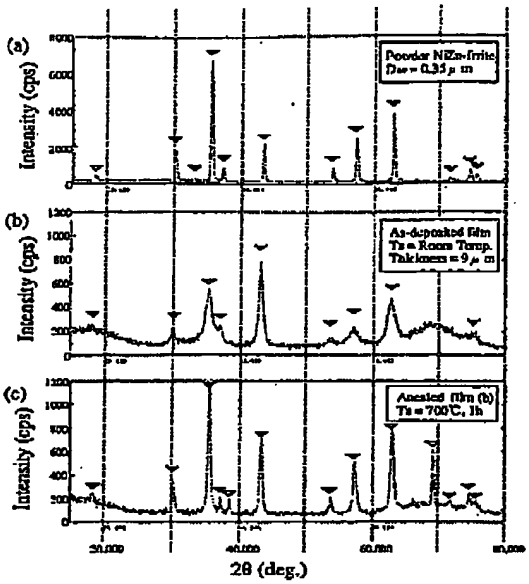

Figure 5. Comparison of XRD pattern of NiZn ferrite.

(b), (c) are for raw-powder, as-deposited at room temperature, annealed at 500℃ PZT, and bulk PZT. Fig. 5 (a), (b), (c) are for raw-powder, as-deposited at room temperature, annealed at 700℃ NiZn ferrite. Fig. 6 (a), (b), (c) are for raw-powder, as-deposited at room temperature, annealed at 650℃ TiO2. The crystal structures of each material deposited film are spectra phases similar to raw-powder; A perovskite structure remained in the as-deposited PZT film, a spinel structure remained in the as-deposited NiZn ferrite film, and an anastuse structure remained in the as-deposited TiO2 film. However, broadering of the spectra and slight shifting of the spectra angle were observed. Moreover, the PZT and TiO2 films have randomly oriented polycrystal structures, but in case of the NiZn ferrite shown in Fig.5 (b), the orientation was

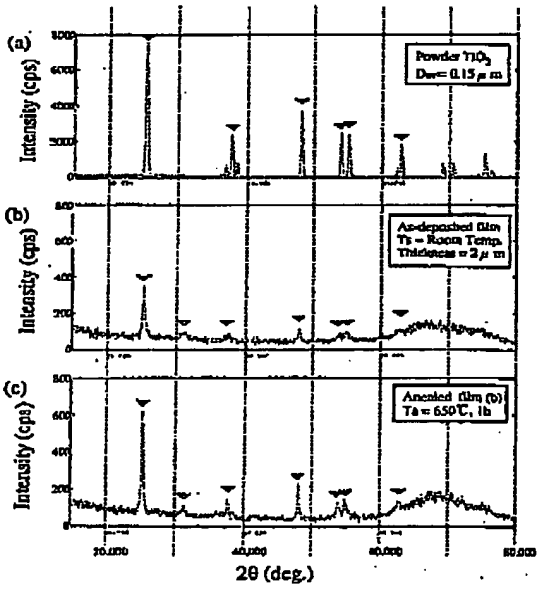

Figure 6. Comparison of XRD pattern of TiO2.

slightly changed. Because the grain size of all raw materials is under 0.3 μ m, small crystallite size of the film or their ununiform distortion during the deposition might be the reason of the slight changes between the raw-powder and the deposited film spectra. After annealing, each spectra of the deposited film in Fig.4 (c), Fig.5 (c), Fig.6 (c) has better sharpness than those of as-deposited films in Fig.4 (b), Fin.5 (b), Fig.6 (b), and was the same or very close to each spectra of raw-powder.

2.4 Ferroelectric property of PZT thick film

(a) As-deposited at room temprature

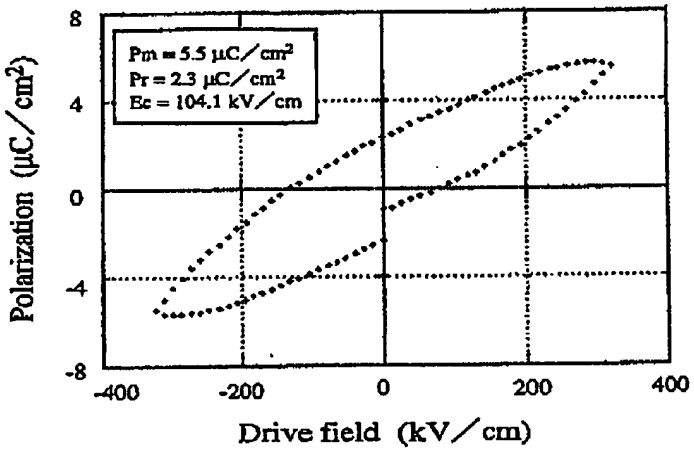

(b) After anealing at 650℃ for 1h

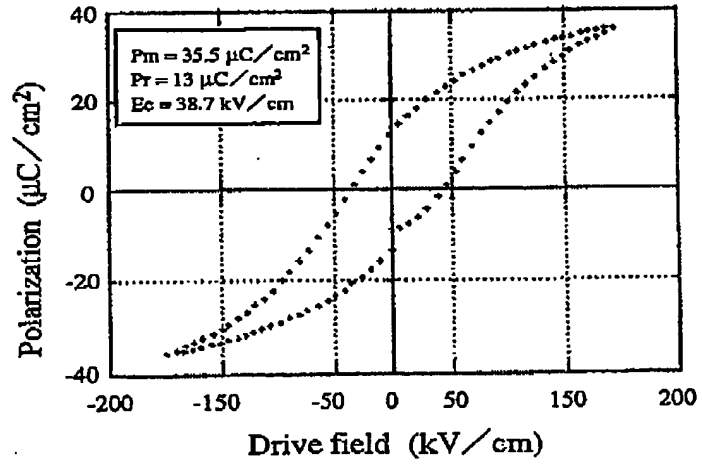

Figure 7. Comparison of the P-E hyateresis loop of the deposited PZT film before and after anealing.

Figures 7(a), (b) show the P-E hysteresis loop for the PZT thick film with thickness of 20 μ m without poling, (a) is for as-deposited film, and (b) is annealed at 650℃, for 1h (heating and cooling speed was ± 300℃／h). The as-deposited sample on the SUS substrate at the room temperature has a ferroelectricity. But the measured remnant polarization of about 2.3 μ C／cm², and the saturation polarization of 5.5 μ C／cm² were very lower than for bulk PZT, and the coercive field of 100 kV／cm was higher than that for the bulk. On the other hand, the breakdown voltage was over 250kV／cm and enough for MEMS applications.

To confirm the piezoelectric character of the as-deposited film, basic actuator elements (beams and membranes) have been structured and covered by PZT. The static deflection of the beam is measured directly by laser-interferometer, and indirectly by the deflection of a reflected laser beam. The calculation uses the analogy between piezoelectrically and thermally induced strain in bimorph structures. The applied assumptions and equations are explained in other reference[10]. As the results, the piezoelectric constant (d_{31}) of as-deposition sample after poling at about 350℃ and applying electrical field continuously until complete cooling down was estimated to -20 to -30 × 10^{-12} C／N. Such a poor property may be explained by low level of the crystallinity. This is confirmed by the XRD observations.

For the sample after anealing, the remnant polarization reached 13 μ C／cm² and the saturation polarization of 35.5 μ C／cm² were improved, and the coercive field of 38.7 kV／cm was drastically decreased. That means the annealing of the film after deposition was effective for improvement of electrical properties. The electrical properties and process temperature were close to the sol-gel driven PZT thin films for MEMS applications[11].

3. CONCLUSION

It was confirmed, not only for PZT but also for other ceramics material such as NiZn ferrite and TiO2, that the as-deposited films by GDM at room temperature have randomly oriented polycrystal structure, preserving the crystal structure of the raw-materials. The deposited films have good adhesion force on the Si and SUS substrates and density close to the bulk ceramics. We think that these results might in the possibility of cramic film formation at low temperature, what is very important for some applications. For example, in case of TiO2 ceramics, recently the problem of fixation on a substrate becomes very important for the application of photocatalyst[12].

Electrical properties of the as-deposited PZT film at room temperature were very poor. Probably it is because of small crystal size of the as-deposited films, or existence of the

internal stress inside of the deposited film structures after the deposition. After anealing at 650℃, crystallinity and electrical property of the film were drastically improved and became almost the same as in the sol-gel driven PZT thin films for MEMS applications. Process of thick PZT film fabrication by this method is much easier and faster than by any of conventional methods.

In the future, we have to make clear the deposition mechanism of ceramic materials and to develop a new method of generation of high quality particle beam for improvement of the film quality and decreasing the process temperature.

ACKNOWLEDGMENTS

The author is grateful to assistant professor of Tohoku Univ. Dr. M. Yamaguchi for discussions of the applications for magnetics and Dr. M. Ichiki, Dr. A. Schroth, R. Maeda, Dr. N. Minami, and Dr. O. Ryabov for their advice and technical assistance in characteristic measurements.

REFERENCES

[1] T. Ide, Y. Mori, I. Konta, N. Ikawa, and H. Yagi : J. Prec.Eng.Jpn.,57, 5, 143 (1991).
[2] S. Kasyu, E.Fuchita, T. Manabe, and C. Hayashi : Jpn.J.Appl.Phys. 23, L910 (1984).
[3] N. P. Rao et al. : J. Aerosol Sci., 29, 5/6, 707 (1998).
[4] Massood T. Azar : MICROACTUATORS, (Kluwer Academic Publishers ,1998).
[5] J.Akedo, M.Ichiki, K. Kikuchi, and R.Maeda: IEEE Proceedings of MEMS`97, Nagoya, Japan, January 26-30, 145 (1997).
[6] H. Adachi, Y. Kuroda, T. Imahashi, and K. Yanagisawa : Jpn.J.Appl.Phys., 36, P1,3,1159 (1997).
[7] J.Akedo, M.Ichiki, K. Kikuchi, and R.Maeda : Sensors & Actuators A-Phys., 69, 106 (1998) .
[8] A. Schroth, R. Maeda, J. Akedo and M. Ichiki : Jpn. J. Appl. Phys., 37, P1- 9B, 3167 (1998).
[9] J.Akedo, M.Ichiki, K. Kikuchi, and R.Maeda: Proceedings of Micro MAT`97, Berlin, Germany, April 16-18, 614 (1997).
[10] A. Schroth : Thesis, Dresden University of technology, Germany (1996).
[11] C.P.Araujo et al. : FERROELECTRIC THIN FILMS: SYNTHESIS AND BASIC PROPERTIES, (Gordon and Breach Publishers, 1996).
[12] T. Yashimoto : Kougyou Zairyou, 45, 10, 62 (1997).

This Page is Inserted by IFW Indexing and Scanning Operations and is not part of the Official Record

BEST AVAILABLE IMAGES

Defective images within this document are accurate representations of the original documents submitted by the applicant.

Defects in the images include but are not limited to the items checked:

- ☐ BLACK BORDERS
- ☐ IMAGE CUT OFF AT TOP, BOTTOM OR SIDES
- ☐ FADED TEXT OR DRAWING
- ☐ BLURRED OR ILLEGIBLE TEXT OR DRAWING
- ☐ SKEWED/SLANTED IMAGES
- ☐ COLOR OR BLACK AND WHITE PHOTOGRAPHS
- ☐ GRAY SCALE DOCUMENTS
- ☐ LINES OR MARKS ON ORIGINAL DOCUMENT
- ☐ REFERENCE(S) OR EXHIBIT(S) SUBMITTED ARE POOR QUALITY
- ☐ OTHER: _____

IMAGES ARE BEST AVAILABLE COPY.
As rescanning these documents will not correct the image problems checked, please do not report these problems to the IFW Image Problem Mailbox.